Chemistry—Methods

Research Article
doi.org/10.1002/cmtd.202400089

Chemistry Europe
European Chemical Societies Publishing

www.chemistrymethods.org

Real-Time *In Situ* Raman Monitoring of Photomechanochemical Reactions

Ivica Cvrtila,[a] Vjekoslav Štrukil,*[a] Marija Alešković,[a] Ivan Kulcsár,[a] Tomislav Mrla,[a] Evelina Colacino,[b] and Ivan Halasz*[a]

In its ongoing development, mechanochemistry is becoming equipped with additional energy inputs such as light. In this work we demonstrate a proof-of-principle setup for real-time *in situ* Raman monitoring of photomechanochemical reactions. Using photoisomerization of azobenzenes, and photolysis of adamantane diazirine as model reactions, we show that multiple photoisomerization cycles can be performed and monitored in a ball mill, and highlight reaction selectivity that can be achieved by photomechanochemistry.

Recent development of mechanochemistry shows a strong incentive to explore its combination with energy input in forms other than mechanical force, such as sound, electricity, or irradiation.[1,2] Light is particularly interesting as it offers direct introduction of energy into the reaction system, as well as a superior level of control over the dynamics of energy input. Among the used wavelengths, UV irradiation is experiencing renewed interest thanks to the development of UV LED sources.[3] Besides, there is an extensive body of knowledge of photochemistry not only in solution, but also in the solid state, that may serve for developing photochemistry in a mechanochemical setting.[4–7] The solid state may restrict motion of molecules and could thus affect the distribution of products, which has previously been applied to increase selectivity and yields in *e.g.* the photolysis of diazenes,[8] the synthesis of compounds with vicinal quaternary carbon atoms,[9] or in the preparation of ladderanes.[6] Furthermore, continuous mixing and crystal or particle breaking in a photomechanochemical setup can be expected to facilitate reactions by maintaining the constant exposure of the whole reaction mixture to the irradiating light.[10] Despite these benefits over solution photochemistry or static irradiation of solids, there are not many reports on combining irradiation with mechanochemistry.[10–18] Some of the reasons for such scarcity may be found in the lack of readily available irradiation sources and compatible milling media that would allow for a practical, yet safe coupling of photochemical reactions with high intensity grinding. Additionally, techniques for real-time *in situ* monitoring of such photomechanochemical reactions, crucial for an in-depth understanding of underlying mechanisms, have not been developed, further limiting the research to more demanding and necessarily delayed *ex situ* monitoring.

We approached this challenge by upgrading our previously developed ball milling setup for *in situ* Raman monitoring,[19,20] with a suitable irradiation equipment,[10] in a similar fashion as it had previously been done for tandem monitoring techniques.[21–23] This approach required a few conditions to be met. First, it was necessary for the irradiation sources and the Raman probe to fit together around the reaction vessel, without interfering with, or being obstructed by the oscillating reaction vessel and shaker-mill arms. Second, the reaction vessel must be transparent in the wavelength range of both the irradiation source and the Raman laser, and must also endure milling. Third, due to the heat released by the irradiation source, a means of cooling of the reaction vessel needed to be arranged.

As our model reactions we chose *E*/*Z*-isomerization in the photoswitches azobenzene (**1**) and its derivative 4-methoxyazobenzene (**2**), and the photolysis of adamantane diazirine (**3**) (Scheme 1). Aside from displaying archetypal reversible photo-

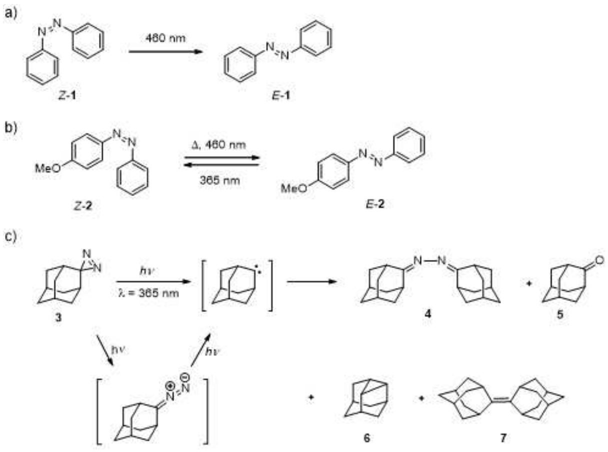

Scheme 1. Photomechanically driven reactions for developing *in situ* monitoring by Raman spectroscopy: a) $Z \rightarrow E$ isomerization of **1**, b) reversible $Z \rightarrow E$ and $E \rightarrow Z$ isomerization of **2**, c) photolysis of **3** in the solid state. In this work **4** is the dominant product.

---

[a] Ruđer Bošković Institute, Zagreb, Croatia
[b] ICGM, CNRS, ENSCM, Univ Montpellier, Montpellier, France

Correspondence: Dr. Vjekoslav Štrukil and Dr. Ivan Halasz, Ruđer Bošković Institute, Bijenička c. 54, Zagreb 10163, Croatia.
Email: vstrukil@irb.hr and ihalasz@irb.hr

Supporting Information for this article is available on the WWW under https://doi.org/10.1002/cmtd.202400089

chemical isomerisation reactions, azobenzenes are interesting as energy storage materials.[24–26] Compound **2** was selected for its absorption maxima at 348 nm for the $E\rightarrow Z$ isomerization, and at 440 nm for the $Z\rightarrow E$ isomerization, both suitable for commonly available LED sources. In contrast, solid *E*-**1** can only be converted to the *Z*-isomer by using laser irradiation,[27] and our attempts to obtain it in the mechanochemical setup, led to no conversion at all. Therefore, *Z*-**1** was prepared in solution, purified by column chromatography and isolated as a pure solid (Figure S2). Only the $Z\rightarrow E$ isomerization was then performed in the photomechanochemical setup.

The photolysis of **3** is a complex reaction producing reactive adamantyl carbene, which can react with a multitude of other compounds, including itself and the starting material. To date, photochemistry of **3** has been thoroughly explored in solution,[28–32] matrix environment,[33,34] and within supramolecular containers, both in solution[35–37] and in the solid state.[38–40] Upon irradiation, diazirines can isomerize into linear diazo compounds,[41] where both can release nitrogen to form the corresponding carbenes.[29–32] Carbene species, depending on the other compounds present in the mixture, can afford various addition products, which have been used *e.g.* in cyclopropanations,[42] preparing organometallics,[43] or for photoaffinity labelling.[44]

For visible light irradiation experiments we used a homemade array of blue LEDs (460 nm), that has already proven to be an efficient means to perform photomechanochemical reactions.[10] For UV irradiation experiments we used an in-house built linear array of UV LEDs (365 nm) equipped with a heat sink, and positioned on a movable aluminium holder mounted on the front panel of the shaker mill (Figure 1, Figure S5). This allowed for precise positioning of the LEDs, and consequently for controlling the intensity of light entering the reaction mixture. Due to their undemanding size, both LED arrays could be mounted simultaneously, *e.g.* to perform monitored photomechanochemical experiments with alternating irradiation sources (Figure S5b–d).

While PMMA jars, commonly used for monitoring mechanochemical reactions, are transparent for visible light, they are not fully compatible with UV irradiation sources.[45] This reduces the choices for the jar material to glasses, including fused silica.

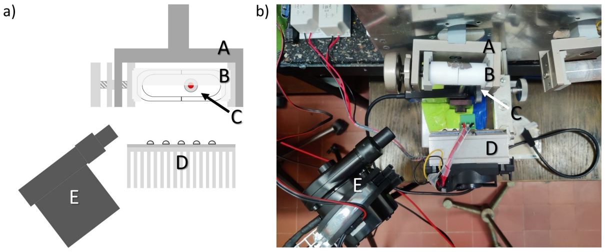

Figure 1. Top view of the setup for monitoring UV photochemical reactions in a mechanochemical setting making use of a horizontal vibrating ball-mill: a) scheme, and b) photograph. A – shaker mill arm, B – quartz jar placed in a Teflon holder, C – Raman probe (pointing upwards), D – UV LED array, E – cooling fan. Due to the orientation of the Teflon holder opening towards the Raman probe and the UV source, the jar inside the holder is not visible on the photograph.

The first part of experiments, with azobenzene, was performed using custom-made glass jars (Figure S4a) that were carefully mounted onto shaker mill arms to avoid crushing and displacement during the experiments. Since laboratory glass has a broad maximum and two relatively sharp peaks in its Raman spectrum, all overlapping with typical signals for organic functional groups (Figure S6a), for later experiments we switched to quartz glass, which has only a broad, low-intensity, maximum between 2500 and 3500 cm^{-1} (Figure S6b). Additionally, a special Teflon holder (Figure S4c) was constructed to facilitate mounting of the jars onto the shaker mill arms. A single Teflon-coated steel ball (10 mm, 1.6 g) was used in all experiments, and the milling frequency was set to 30 Hz.

Although LEDs are the most efficient light sources today, the heat they release still makes up the majority of their energy output.[46] This means that, along with UV photons, the irradiated jar will also receive heat in the form of IR irradiation. In our setup, the LED array (5×2–3 W optical power) at the minimal distance from the jar (2.1 cm) increased the temperature of the outer surface of the jar to 94 °C. Ideally, IR irradiation could be prevented from reaching the jar using a quartz screen with circulating water. However, this is sterically cumbersome, so we opted for a cooling fan. This worked satisfactorily, as the fan reduced the outer surface temperature of the jar to 36 °C at the minimal distance from LEDs to the jar, and to 27 °C (which is 4 degrees above the jar temperature without irradiation) at a higher distance (6.0 cm) (Figure S8).

In the $Z\rightarrow E$ photoisomerization of **1** (Scheme 1a), induced by blue light (460 nm), it was noticed that the compound readily sticks to glass of the reaction jar, which precluded monitoring. To improve the rheological properties[47] of the reaction mixture, 80 mg of **1** was mixed with up to 5 time in mass of anhydrous Na_2SO_4, finally resulting in a free-flowing powder. A 2D data plot of the time-resolved Raman spectra shows a smooth transition from the *Z*-isomer to the *E*-isomer in about an hour (Figure 2a). For a more precise picture, intensities of characteristic Raman signals for the starting material *E*-**1** (156 cm^{-1}, phonon area) and the product *Z*-**1** (1428 cm^{-1}, related to $-N{=}N-$ vibrations) were plotted as a function of time (Figure 2b, see also Figures S10–S14), indicating that there are no other species present during the photoisomerisation.

We continued with the $E\rightarrow Z$ and the $Z\rightarrow E$ photoisomerization of **2** (Scheme 1b), using 365 nm UV irradiation for the $E\rightarrow Z$ isomerisation, and the 460 nm blue light for the reverse process. Acceptable rheological behaviour was now reached by mixing 50 mg of **2** with ten times as much Na_2SO_4. Photomelting[48] of **2** during irradiation changed the appearance of the reaction mixture to darker shade of orange, and to more sticky particles, but the material in the jar remained powdery.

The $E\rightarrow Z$ photoisomerisation exhibited a rapid transformation from the pure *E*-isomer into a photostationary mixture with predominately the *Z*-isomer ($E:Z=14:86$, based on NMR), in ten to fifteen minutes, depending on the distance of the LEDs from the jar (Figure 3, see also Figures S15–S17), clearly indicating that the intensity of the radiation delivered to the sample influences the rate of the photochemical switching. Period of milling without irradiation (first 2 min in Figure 3a,

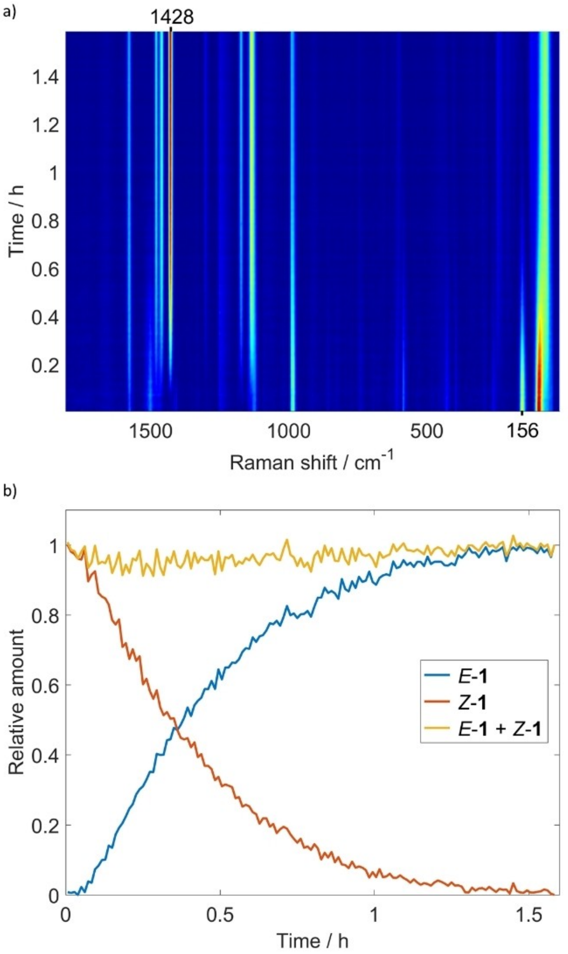

Figure 2. $Z \rightarrow E$ photoisomerization of **1** monitored by *in situ* Raman spectroscopy: a) time-resolved 2D Raman plot, b) kinetic profile of the reaction, based on peak intensities at 156 cm^{-1} (*E*-**1**) and 1428 cm^{-1} (*Z*-**1**) normalized against the Na_2SO_4 signal at 991 cm^{-1} (Figure S7).

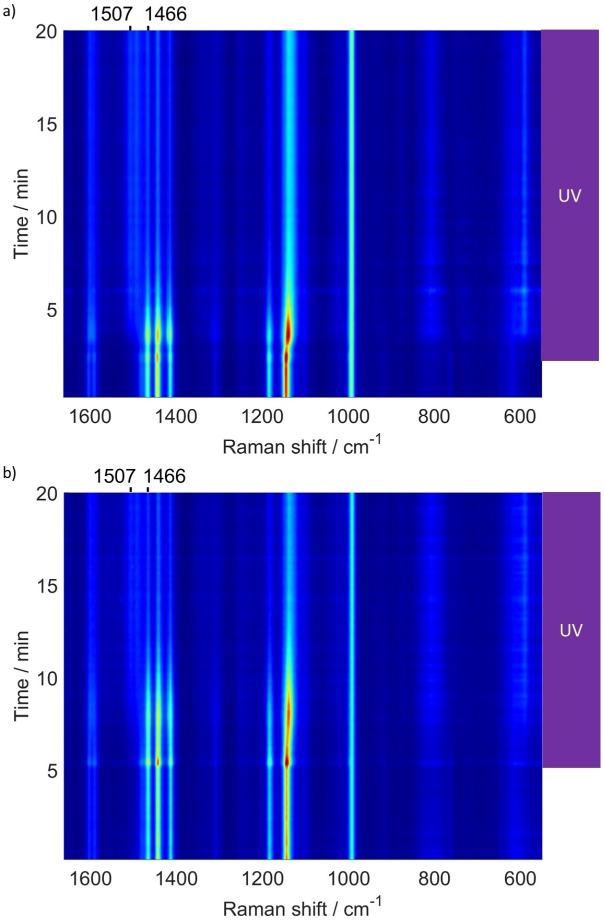

Figure 3. Time-resolved 2D plots for Raman-monitored $E \rightarrow Z$ photoisomerization of **2** in a mechanochemical setting: a) UV LEDs 2.1 cm away from the jar, b) UV LEDs 5.1 cm away from the jar. Irradiation indicated on the right sides of plots by purple shading.

and first 5 min in Figure 3b) produced no changes in the Raman spectra. On the other hand, milling the irradiated mixture in dark led to slow thermal isomerization (Figures S23–S30), with isomerization rates similar to those observed in standing solid samples.[48]

Next, we hypothesised that alternating $E \rightarrow Z$ and $Z \rightarrow E$ photoisomerizations of **2**, using intermittently the UV and the blue sources, could be accomplished. Having mounted both irradiation sources (Figures S5, S31–33), we performed three switching cycles under continuous Raman monitoring (Figure 4) demonstrating also, for the first time, that multiple photoswitching cycles (from predominantly *E*-**1** to predominantly *Z*-**1**) can be achieved during ball milling, maintaining high efficiency in each cycle.

Finally, we performed Raman monitoring of the photolysis of the diazirine **3** in the solid state using UV LED source. Again, sticking of the reactant to the glass walls of the jar was prevented by adding up to ten times the amount of anhydrous Na_2SO_4 to 50 or 100 mg of **3**. Monitoring the irradiation of **3** showed a rapid transformation, with azine **4** (Scheme 1c) being the dominant product, and the reaction completed in a few minutes (Figures S41–S44). Similar reaction times have been observed in solution, albeit with much stronger irradiation sources.[37] Sources such as mercury lamps required irradiation times in hours.[30] Notably, solvents must be dried and deaerated before use in photochemical reactions. We also conducted the purely mechanochemical experiment, without UV irradiation (Figure S37), and have fully recovered the starting diazirine **3**, ruling out the possibility that a carbene was formed due to milling.

To slow down the photoreaction, we covered 4 out of 5 LEDs of our UV source, resulting in the reaction being complete in about 15 minutes (Figure 5a, see also Figures S45 and S46). The reaction profile is typical for a solid-state reaction (Figure 5b), except for the strongest product signal at 1620 cm^{-1}, which exhibits a different increase in intensity (Figure S47) from any other signal. In particular, the two-step growth and a subtle shift of the band maximum from 1619 cm^{-1} to 1614 cm^{-1}. Since this signal is most likely related to the C=N vibrations in **4**,[28] its behaviour may stem either from isomerization around the N–N bond in **4**, or a phase transition that involves changes in conformation.

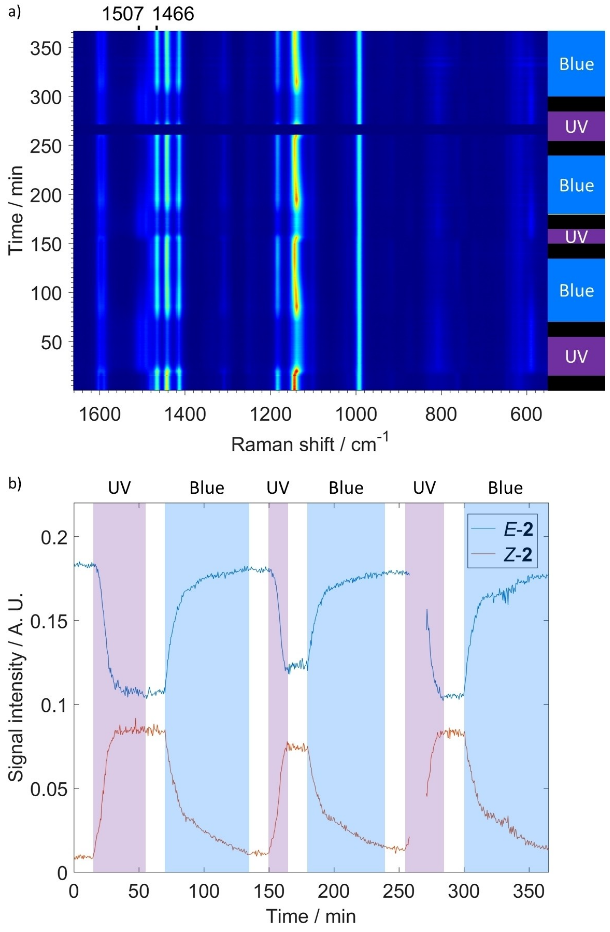

Figure 4. Switching cycles on **2** in a mechanochemical setting, using 365 nm and 460 nm irradiation, respectively: a) time-resolved 2D plot, and b) selected Raman signal intensities of *E*-**2** (1466 cm^{-1}) and *Z*-**2** (1507 cm^{-1}) over time. Data affected by a temporary malfunction of the Raman probe (260–270 min) not shown.

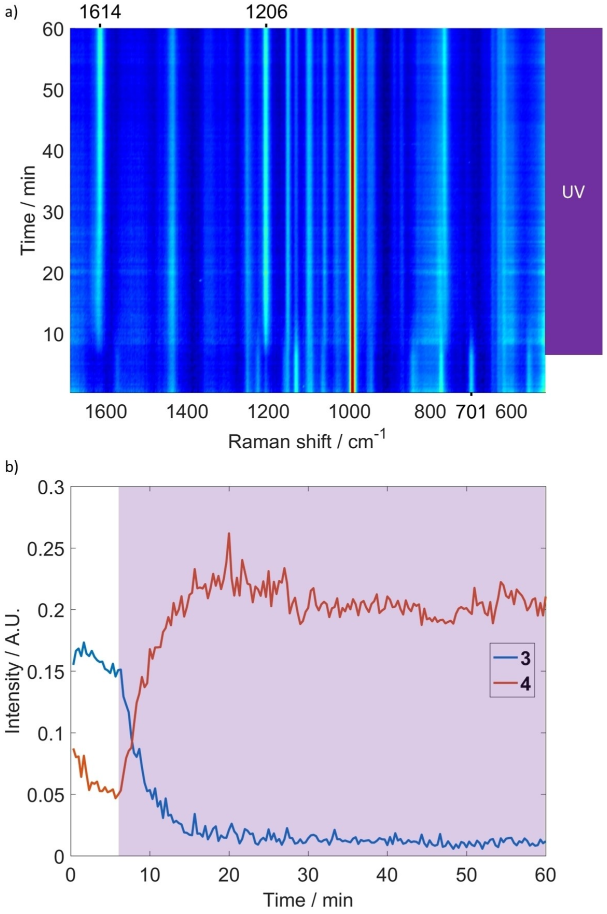

Figure 5. Photolysis of adamantane diazirine **3** using a single UV LED at 6.0 cm distance from jar: a) time-resolved 2D plot; b) selected Raman signal intensities of the starting material (701 cm^{-1}) and the major product (1206 cm^{-1}) as a function of time. Irradiation period is denoted by purple shading.

^{1}H NMR analysis of the product mixtures (Figures S38, S39) revealed that azine **4** is formed as the dominant product (about 70%, similar to highest previously reported yields in solution[28,41]), with a minor amount of adamantanone **5**. Additionally, characteristic chemical shifts indicate dehydroadamantane **6** and biadamantilydene **7** as possible by-products (Scheme 1c). The by-products were also confirmed by GC-MS (Figure S40), but in much smaller proportions, possibly due to their high volatility and less ready ionization. Extraction from the reaction mixtures, followed by chromatographic purification, yielded 39% of **4** and 15% of **5**. A possible cause for lower isolated yield is degradation during isolation.

Previous literature reports provide an insight into the mechanism of formation of isolated products. In the case of **4**, its formation is explained by a bimolecular reaction of the carbene with the diazo intermediate,[28,31,32,49] or the starting **3**.[50] Ketone **5** is known to form in the reaction of intermediate carbene with atmospheric O_2.[51] We have observed, however, in a separate experiment, performed in an inert atmosphere, that the yield of **5** remained the same as when oxygen was present (see SI, Figures S48, S49, and Table S3), suggesting that species other than O_2, such as Na_2SO_4 present in the mixture, could be sources of oxygen for this reaction. On the other hand, **6** is formed by intramolecular 1,3 C–H insertion of the carbene intermediate,[29–32] while **7** is formed directly from it. Strong selectivity of the solid-state photolysis of **3** for **4** rather than **7** is most likely due to high reactivity of the nascent carbene, as the first ready co-reactant molecule to encounter is the starting material **3**, with **4** being significantly more inert. Additionally, the photomechanochemical reaction of diazirine **3** without a solvent prevented formation of by-products resulting from carbene insertion into the solvent molecule.

In summary, we show that Raman monitoring of photochemical reactions in a mechanochemical setting can be efficiently performed, including photoisomerisations as well as photolysis reactions. Photoisomerization of azobenzenes shows that, by using different irradiation sources, multiple back-and-forth isomerization cycles can be efficiently performed in a ball mill, and that established photochemical reactions in solution are likely to exhibit different product selectivity in a mechanochemical environment. This sets path for a more systematic approach to study photochemistry in the solid state and creates opportunities for extending the complex photochemistry of organic compounds to the mechanochemical ball milling environment.

Acknowledgments

We are grateful to dr. Nikola Basarić for lending us the 365 nm lamp for preliminary experiments and Dr Martin Lončarić for spectrum measurements of the lamp. We are also grateful to Mario Pajić and Leonarda Vugrin for useful suggestions regarding data processing and validation. We are thankful to the Croatian Science Foundation for funding through grant No. IP-2020-02-1419.

Conflict of Interests

The authors declare no conflict of interest.

Data Availability Statement

The data that support the findings of this study are available from the corresponding author upon reasonable request.

Keywords: mechanochemistry · *in situ*monitoring · ball milling · photolysis · photoswitching

[1] T. Friščić, C. Mottillo, H. M. Titi, *Angew. Chem. Int. Ed.* **2020**, *59*, 1018–1029.
[2] V. Martinez, T. Stolar, B. Karadeniz, I. Brekalo, K. Užarević, *Nat. Chem. Rev.* **2022**, *7*, 51–65.
[3] G. Goti, K. Manal, J. Sivaguru, L. Dell'Amico, *Nat. Chem.* **2024**, *16*, 684–692.
[4] G. M. J. Schmidt, D. Ginsburg, M. D. Cohen, J. D. Dunitz, D. Ginsburg, Eds., *Solid State Photochemistry: A Collection of Papers Describing a Symbiotic Relationship between X-Ray Crystallography and Synthetic Organic Photochemistry*, Verl. Chemie, Weinheim, **1976**.
[5] F. Toda, Ed., *Organic Solid State Reactions*, Springer Berlin Heidelberg, Berlin, Heidelberg, **2005**.
[6] L. R. MacGillivray, G. S. Papaefstathiou, T. Friščić, T. D. Hamilton, D.-K. Bučar, Q. Chu, D. B. Varshney, I. G. Georgiev, *Acc. Chem. Res.* **2008**, *41*, 280–291.
[7] M. Irie, *Diarylethene Molecular Photoswitches: Concepts and Functionalities*, Wiley-VCH, Weinheim, Germany, **2021**.
[8] P. A. Hoijemberg, S. D. Karlen, C. N. Sanramé, P. F. Aramendía, M. A. García-Garibay, *Photochem. Photobiol. Sci.* **2009**, *8*, 961–969.
[9] J. J. Dotson, S. Perez-Estrada, M. A. Garcia-Garibay, *J. Am. Chem. Soc.* **2018**, *140*, 8359–8371.
[10] V. Štrukil, I. Sajko, *Chem. Commun.* **2017**, *53*, 9101–9104.
[11] F. Toda, S. Hirano, S. Toyota, *Heterocycles* **2004**, *64*, 383.
[12] A. N. Sokolov, D. Bučar, J. Baltrusaitis, S. X. Gu, L. R. MacGillivray, *Angew. Chem. Int. Ed.* **2010**, *49*, 4273–4277.
[13] J. Stojaković, B. S. Farris, L. R. MacGillivray, *Chem. Commun.* **2012**, *48*, 7958.
[14] M. Obst, B. König, *Beilstein J. Org. Chem.* **2016**, *12*, 2358–2363.
[15] J. G. Hernández, *Beilstein J. Org. Chem.* **2017**, *13*, 1463–1469.
[16] D. M. Baier, C. Spula, S. Fanenstich, S. Grätz, L. Borchardt, *Angew. Chem. Int. Ed.* **2023**, *62*, e202218719.
[17] S. Biswas, S. Banerjee, M. A. Shlain, A. A. Bardin, R. V. Ulijn, B. L. Nannenga, A. M. Rappe, A. B. Braunschweig, *Faraday Discuss.* **2023**, *241*, 266–277.
[18] F. Millward, E. Zysman-Colman, *Angew. Chem. Int. Ed.* **2024**, *63*, e202316169.
[19] D. Gracin, V. Štrukil, T. Friščić, I. Halasz, K. Užarević, *Angew. Chem. Int. Ed.* **2014**, *53*, 6193–6197.
[20] S. Lukin, K. Užarević, I. Halasz, *Nat. Protoc.* **2021**, *16*, 3492–3521.
[21] L. Batzdorf, F. Fischer, M. Wilke, K. Wenzel, F. Emmerling, *Angew. Chem. Int. Ed.* **2015**, *54*, 1799–1802.
[22] S. Lukin, T. Stolar, M. Tireli, M. V. Blanco, D. Babić, T. Friščić, K. Užarević, I. Halasz, *Chem. Eur. J.* **2017**, *23*, 13941–13949.
[23] P. A. Julien, M. Arhangelskis, L. S. Germann, M. Etter, R. E. Dinnebier, A. J. Morris, T. Friščić, *Chem. Sci.* **2023**, *14*, 12121–12132.
[24] K. Griffiths, N. R. Halcovitch, J. M. Griffin, *Chem. Sci.* **2022**, *13*, 3014–3019.
[25] H. P. Q. Nguyen, A. Mukherjee, J. Usuba, J. Wan, G. G. D. Han, *Chem. Sci.* **2024**, *15*, 18846–18854.
[26] K. Griffiths, N. R. Halcovitch, J. M. Griffin, *New J. Chem.* **2022**, *46*, 4057–4061.
[27] U. Bhattacharjee, D. Freppon, L. Men, J. Vela, E. A. Smith, J. W. Petrich, *ChemPhysChem* **2017**, *18*, 2526–2532.
[28] S. D. Isaev, A. G. Yurchenko, F. N. Stepanov, G. G. Kolyada, S. S. Novikov, N. F. Karpenko, *Zh. Org. Khim.* **1973**, *9*, 724–727.
[29] R. A. Moss, M. J. Chang, *Tetrahedron Lett.* **1981**, *22*, 3749–3752.
[30] S. D. Isaev, V. P. Sherstyuk, O. F. Kozlov, V. V. Skripkin, I. Yanku, *Theor. Exp. Chem.* **1991**, *27*, 192–199.
[31] S. Morgan, J. E. Jackson, M. S. Platz, *J. Am. Chem. Soc.* **1991**, *113*, 2782–2783.
[32] R. Bonneau, B. Hellrung, M. T. H. Liu, J. Wirz, *J. Photochem. Photobiol. Chem.* **1998**, *116*, 9–19.
[33] T. Bally, S. Matzinger, L. Truttmann, M. S. Platz, S. Morgan, *Angew. Chem. Int. Ed. Engl.* **1994**, *33*, 1964–1966.
[34] H. Tomioka, *Res. Chem. Intermed.* **1994**, *20*, 605–634.
[35] S. Gupta, R. Choudhury, D. Krois, G. Wagner, U. H. Brinker, V. Ramamurthy, *Org. Lett.* **2011**, *13*, 6074–6077.
[36] S. Gupta, R. Choudhury, D. Krois, U. H. Brinker, V. Ramamurthy, *J. Org. Chem.* **2012**, *77*, 5155–5160.
[37] T. Šumanovac, M. Alešković, M. Šekutor, M. Matković, T. Baron, K. Mlinarić-Majerski, C. Bohne, N. Basarić, *Photochem. Photobiol. Sci.* **2019**, *18*, 1806–1822.
[38] U. H. Brinker, R. Buchkremer, M. Kolodziejczyk, R. Kupfer, M. Rosenberg, M. D. Poliks, M. Orlando, M. L. Gross, *Angew. Chem. Int. Ed. Engl.* **1993**, *32*, 1344–1345.
[39] M. D. Poliks, U. H. Brinker, R. Kupfer, *J. Am. Chem. Soc.* **1994**, *116*, 7393–7398.
[40] D. Krois, L. Brecker, A. Werner, U. H. Brinker, *Adv. Synth. Catal.* **2004**, *346*, 1367–1374.
[41] R. Bonneau, M. T. H. Liu, *J. Am. Chem. Soc.* **1996**, *118*, 7229–7230.
[42] T. Rogge, Q. Zhou, N. J. Porter, F. H. Arnold, K. N. Houk, *J. Am. Chem. Soc.* **2024**, *146*, 2959–2966.
[43] P. De Frémont, N. Marion, S. P. Nolan, *Coord. Chem. Rev.* **2009**, *253*, 862–892.
[44] L. Dubinsky, B. P. Krom, M. M. Meijler, *Bioorg. Med. Chem.* **2012**, *20*, 554–570.
[45] K. G. D. C. Monsores, A. O. D. Silva, S. D. S. A. Oliveira, J. G. P. Rodrigues, R. P. Weber, *J. Mater. Res. Technol.* **2019**, *8*, 3713–3718.
[46] K. Hölz, J. Lietard, M. M. Somoza, *ACS Sustainable Chem. Eng.* **2017**, *5*, 828–834.
[47] L. Konnert, A. Gauliard, F. Lamaty, J. Martinez, E. Colacino, *ACS Sustainable Chem. Eng.* **2013**, *1*, 1186–1191.
[48] J. Hu, S. Huang, M. Yu, H. Yu, *Adv. Energy Mater.* **2019**, *9*, 1901363.
[49] R. A. Moss, M. J. Chang, *Tetrahedron Lett.* **1981**, *22*, 3749–3752.
[50] G. V. Shustov, M. T. H. Liu, K. N. Houk, *Can. J. Chem.* **1999**, *77*, 540–549 .
[51] H. Tomioka, *Triplet Carbenes*, Hoboken, NJ, **2004**.
[52] L. Duarte, R. Fausto, I. Reva, *Phys. Chem. Chem. Phys.* **2014**, *16*, 16919–16930.
[53] A. Mostad, C. Romming, *Acta Chem. Scand.* **1971**, *25*, 3561–3568.
[54] A. P. Marchand, K. A. Kumar, K. Mlinarić-Majerski, J. Veljković, *Tetrahedron* **1998**, *54*, 15105–15112.
[55] V. M. Kolb, A. C. Kuffel, H. O. Spiwek, T. E. Janota, *J. Org. Chem.* **1989**, *54*, 2771–2775.
[56] N. Bian, M. Jones, *J. Am. Chem. Soc.* **1995**, *117*, 8957–8961.
[57] M. P. Fleming, J. E. McMurry, *Org. Synth.* **1981**, *60*, 113.

Manuscript received: December 20, 2024
Version of record online: January 31, 2025